Recent Progress in Lunar Topographic Mapping using OrbiterMapper and LROC NAC Stereo Images. Ron Li[1], Liwen Lin[1], Wei Wang[1], Justin Crawford[1], Xuelian Meng[1], Shaojun He[1], Mark Robinson[2], and the LROC Science Team. [1]Mapping and GIS Laboratory, CEEGS, The Ohio State University, 470 Hitchcock Hall, 2070 Neil Avenue, Columbus, OH 43210-1275, [li.282, lin.1128]@osu.edu. [2]Arizona State University.

Introduction: As one of seven remote-sensing instruments carried onboard the Lunar Reconnaissance Orbiter (LRO), the Lunar Reconnaissance Orbiter Camera (LROC) system has two NAC (Narrow Angle Camera) cameras that acquire high-resolution imagery for the assessment of meter-scale features on the lunar surface [1, 2]. Stereo pairs for 3D topographic mapping are formed by combining images from two or more adjacent orbits (cross-track stereo). The Ohio State University (Ohio State) has developed an OrbiterMapper software package to generate topographic products using LROC NAC data in support of the science goals of the LRO mission.

Development of OrbiterMapper: OrbiterMapper is a software application package that photogrammetrically processes lunar and Martian orbital imagery for 3D topographic generation. The entire process can be divided into two major sections: (1) image processing that primarily involves image preprocessing and a hierarchical coarse-to-fine hierarchical matching process [3] for the extraction of accurate dense matching; and (2) geometric processing that mainly includes boresight calibration and bundle adjustment to remove the geometric inconsistencies in the Exterior Orientation (EO) parameters among stereo orbits [4]. With dense matching points from image processing and bundle-adjusted EO parameters from geometric processing, highly accurate 3D terrain models can be constructed.

The current version of OrbiterMapper includes several significant improvements over previous versions. These improvements include two rounds of grid matching for more reliable matching and three-fold matching along seam lines in order to decrease seam inconsistency in the DEM overlapping area.

Two rounds of grid matching are used to overcome the problem of small artificial bumps (1 m ~ 2 m) due to mismatching. These bumps usually are located in smooth areas having steep slopes, areas that have large image distortion between stereo images caused by a large slew angles. When performing grid matching in these areas, matching points from previous levels have difficulties in providing accurate prediction of matched points for least-squares matching, which would cause mismatching and, in turn, bumps in the terrain if grid matching is performed only once. Therefore, the grid-matching step is performed twice. The result of the first round of grid matching provides information for eliminating mismatching points, consequently, is capable of offering good predictions and dense points for the second round. Figure 1 shows an example of the improvement from two rounds of grid matching on the Tsiolkovskiy Crater DEM.

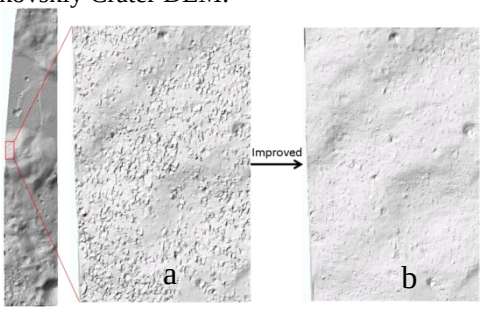

Figure 1. Tsiolkovskiy Crater DEM: a) result from 1 round of grid matching compared with b) the improvement made by 2 rounds of grid matching.

Another reason for the occurrence of small bumps on the DEM could be a narrow range of pixel values over an image area. A small range of pixel values means low contrast and obscure features in the image, which could cause a slight disturbance of accuracy in least-squares matching and, thus, lead to small artificial bumps. These artificial bumps probably would mislead scientific observations and analysis of the lunar surface. We find that performing suitable image stretching and enhancement in a local area to increase the image contrast and distinctness of features can effectively remove these artificial bumps (0.1 ~ 0.4 m). This is illustrated in Figure 2, which shows a sample region from the DEM of stereo pair images M161252379 and M161245596.

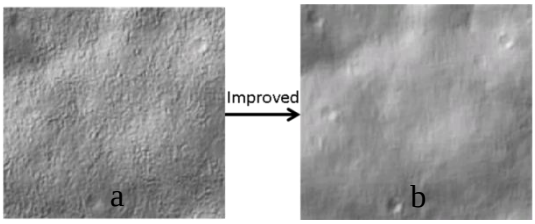

Figure 2. One Sample Region showing improvement from image stretching and enhancement for bump removal: a) before and b) after local stretching and enhancement.

Although the geometric inconsistencies among EOs of stereo orbits could be improved by geometric processing, conspicuous seam lines may exist along the DEM overlapping area of two NAC CCDs. In a previous version of OrbiterMapper, the 3D coordinates

of the points along the seam lines, like other points in the DEM, were derived through the intersection of two matching points in two-orbit images. However, the points in the seam lines can actually have triple matching points: two inter-strip points located in the overlapping area of two CCDs in one orbit, and a third one in the other orbit's CCD. If all of these three matching points can be used for intersection of the ground point, then it is possible to distribute the remaining geometric inconsistencies (about a half pixel) to several pixels across the seam line, which would lead to the further alleviation of the seam line. Figure 3 shows an example of this improvement for the Compton Crater site: an almost invisible seam line due to the employment of all three matching points.

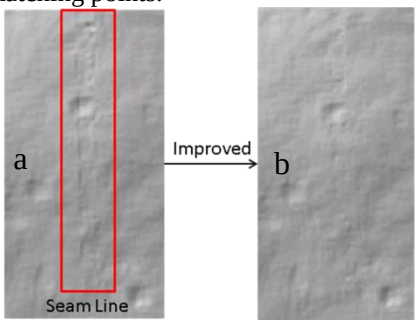

Figure 3. Example of the improvement of seam lines at the Compton Crater site: a) the original result with visible seam line, and b) improved result.

In addition to these improvements to OrbiterMapper, efforts also are being made for boresight calibration and jitter analysis. Boresight calibration is designed to obtain highly-accurate boresight parameters that describe the relative alignment between two NAC cameras [4]. Currently, we are conducting experiments using two methods for boresight calibration to improve boresight parameters. The first method is to combine the boresight calibration and bundle adjustment together to jointly solve both boresight parameters and EO polynomial parameters. The other method is to consecutively perform bundle adjustment and boresight calibration to separately compute EO polynomial parameters and boresight parameters. In addition, it has been found that some DEMs from NAC stereo imagery are subject to geometric distortions due to spacecraft jitters [3, 5, 6]. This jitter effect is represented as artificial horizontal ripples in the cross-track direction. We are currently working on detecting and modeling the jitter effect in order to eliminate artificial terrains on DEM products.

Topographic Products for Scientific Applications: Since June 2010, OrbiterMapper has been evaluated through a DEM comparison using data covering the Apollo 15 landing site and Tsiolkovskiy Crater. OrbiterMapper has been applied successfully to the generation of 3D lunar terrain for different scientific objectives. To date, we have generated topographic products for more than ten sites, including Compton, Compton-Belkovich, and King Crater. Our products have been used by LRO science team members to study the formation of lunar features such as craters and lunar lobate scarps and to analyze topographic characteristics of targets of interest. Among these products, a considerable number of requests have been for the research of lunar lobate scarps, which are relatively small-scale, discontinuous, linear or curvilinear tectonic landforms with relatively steep scarp faces. The study of lunar lobate scarps, one of the youngest landforms on the moon, can shed light on mechanical clues about the lunar regolith and lithosphere [7, 8]. Recently, we are generating a DEM product of the lobate scarps near Mandel'shtam Crater, a group of scarps that can be viewed as the surface expression of splay faults [9]. Figure 4 shows one sample region of the lobate scarps in this DEM and several elevation profiles across the scarps.

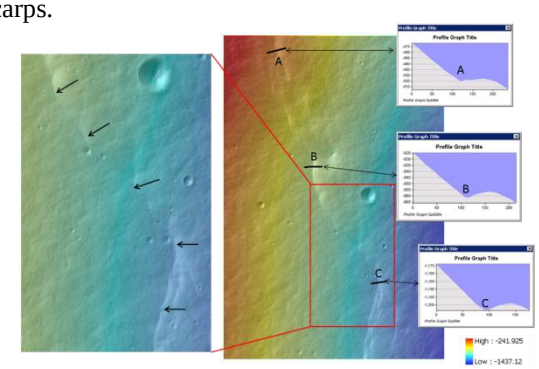

Figure 4. Lobate scarp near Mandel'shtam Crater [stereo pair: M161252379 and M161245596]. A, B, and C are 3 examples of elevation profiles across the scarps.

Acknowledgements: This research is supported by the National Aeronautics and Space Administration under Agreement No. NNX08AR29G issued through the Science Mission Directorate.

References: [1] Robinson, M. S. et al. (2005) *LPSC XXXVI*, Abstract #1576. [2] Robinson, M. S. et al. (2010) *Space Science Reviews*, 150:81-124. [3] Li, R. et al. (2011) *IEEE Transitions on Geoscience and Remote Sensing*, 49(7):2558-2572. [4] Li, R. et al. (2010) *Annual Meeting of LEAG*, Abstract #1595. [5] Mattson, S. et al. (2010) *LPSC XLI*, #1871. [6] Mattson, S. et al. (2011) *LPSC XLII*, Abstract #2756. [7] Banks, M. E. et al. (2011) *LPSC XLII*, Abstract #2779. [8] Watters, T. R. and C. L. Johnson. (2010) in Planetary Tectonics, Cambridge Univ. Press, 121-182. [9] Watters. T.R. et al. (2010) *Science*, 329(5994):936-940.